Seismic traveltime inversion using Metropolis-Hasting method with sigmoidal parameterization

Juarez S. Azevedo[1], Lucas F. Palma[1], Saulo P. Oliveira[2,*], and Wilson M. Figueiró[1]

[1]Federal University of Bahia, [2]Federal University of Paraná.

Abstract

Seismic traveltime tomographic inversion is essential to help estimate the internal structure of the solid earth. For such, we propose to approximate the complex geological structure of a given media based on parameterization by sigmodal functions of discontinuous velocity fields. In addition, we use the Metropolis-Hasting (global-scope) algorithm for the inversion procedure. Through this inversion method, we provide high-resolution estimates of the model's parameters and ensure that the results obtained are in accordance with actual data. Synthetic models are employed to validate the method.

Introduction

Seismic traveltime tomography inversion methods aim to produce a better mapping of geological structures through seismic data processing and interpretation, with an essential contribution to estimate reservoir continuity. However, these methods depend on the choice of parameterization of velocity model (Kissling et al., 2001; Tong et al., 2019) and cannot capture, with desired efficiency, discontinuities in velocity model. Moreover, experiments involving parameterizations with splines and wavelets functions (Michelini and McEvilly, 1991; Cerqueira et al., 2016) have shown that velocity fields can be represented without violating discontinuities.

Several authors have suggested improvements in the process of parameterization of models (Tikhotskii et al., 2011; Evensen and Landrø, 2010; Belhadj et al., 2018). Motivated by these works, we show that, under certain restrictions, a rigorous formulation of the inversion procedure from traveltimes for the discontinuous velocity models is possible in the scope of parameterization through a linear combination of sigmoidal functions (Costarelli and Spigler, 2013; Oliveira et al., 2020). This methodology allows sharp variations of the velocity model without neglecting continuity, besides, it does not need domain decomposition. To this end, we invert the travel times to obtain velocity field and interface structure at the same time using the method of ray tracing.

Realistic models can be better represented by this sigmoidal functions and the ambiguity, commonly present in inversion techniques results, can be reduced if sufficient data is available. Furthermore this kind of parameterization have a good adjustability in the discontinuous model since its approximation strongly depends on the sigmoidal parameter which requires no additional computational cost, especially for complex models whose difficulty in representing the discontinuity by a fine mesh is inherent.

In the inversion procedure we use Metropolis Hasting method (MH) (global scope) (Azevedo et al., 2014) as a Bayesian inversion strategy to minimize the error between observed and computed data, adjusting the model parameters and boundary nodes simultaneously in each iteration. First, an initial set of samples for the MH algorithm is assembled through a small-scale random search generated by the Monte Carlo method, with no prior knowledge of the minimum. We expect that random sequences generated by the Monte Carlo method will improve the performance of the MH method when applied to the initial population. Then, after a certain number of samples, MH method is started from the initial guess in such a way that the distribution of values converges to the desired distribution considering that the candidate point is either accepted or rejected using the acceptance probability.

In this paper, we start with a qualitative 1D geological model and typical velocities values are arbitrated for each layer, extending these results to the two-dimensional case. From then on, a mesh of points is placed over the domain of velocity model, having at each point a horizontal coordinate (which symbolizes the distance on the surface), a vertical coordinate (which symbolizes the depth of the point) and an associated seismic velocity. The number and position of each parameter of the model is made in general and inserted in the data set. Then we use ray tracing to determine traveltimes for a fixed set of ray take-off angles. The results obtained by both experiments were compared with Very Fast Simulated Annealing (VFSA) method.

Model Parameterization

The parameterization of the velocity field is based on the sigmoidal approximation of piecewise-constant functions, which we describe next.

Following the notation of Oliveira et al. (2020), we approximate the one-dimensional velocity field $v(z)$ as

follows:

$$v_a(z) = \sum_{n=-1}^{N} v_n \phi_a\left(\frac{z}{h} - n\right), \quad (1)$$

where the sigmoidal function ϕ_a is defined as

$$\phi_a(x) = \frac{1}{1+e^{-ax}} - \frac{1}{1+e^{-a(x-1)}}, \quad (2)$$

and a represents the parameter that controls the transition between plateaus, which may be smooth or sharp if a is small or large, respectively. This is confirmed by the one-dimensional velocity model shown in Fig. 1.

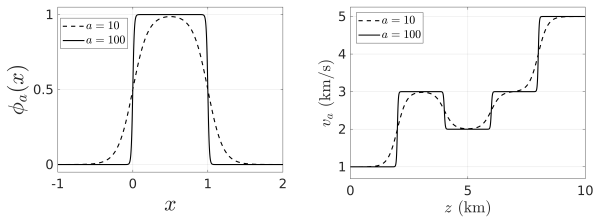

(a) (b)

Figure 1: Sigmoidal scaling function (a) and approximation of a piecewise-constant function (b) with slope parameters a =10 and a =100.

Approximation (1) can also be easily extended to a rectangular domain $[0, L_x] \times [0, L_z]$ with grid points $(x_m, z_n) = (mh_x, nh_z)$, $0 \le m \le N_x$ and $0 \le n \le N_z$, by the following tensor-product expansion:

$$v_a(x,z) = \sum_{n=-1}^{N_z} \sum_{m=-1}^{N_x} v_{m,n} \phi_a\left(\frac{x}{h_x} - m\right) \phi_a\left(\frac{z}{h_z} - n\right), \quad (3)$$

which can be approximated as

$$v_a(x,z) \approx \sum_{i=-1}^{1} \sum_{j=-1}^{1} v_{m_i,n_j} \phi_a\left(\frac{x}{h_x} - m_i\right) \phi_a\left(\frac{z}{h_z} - n_j\right), \quad (4)$$

where $m_i = m+i$, $n_j = n+j$, $(x,z) \in [x_m, x_{m+1}] \times [z_n, z_{n+1}]$ and the summation limits may be modified to guarantee $0 \le m+i \le N_x$ and $0 \le n+j \le N_z$.

Ray tracing in heterogeneous models

The traveltime from source A to receiver B on two-dimensional media can be obtained through the velocity model V solving the following line integral

$$T_{AB} = \int_{\mathbf{l}_{AB}} \frac{1}{v(\mathbf{l})} d\mathbf{l} \quad (5)$$

where $V(\mathbf{l})$ is the (unknown) local velocity along the (unknown) actual ray path $\mathbf{l}_{AB}$ between A and B, which is calculated numerically by the following equation:

$$T_{AB}(x_{N+1}, z_{N+1}) = \sum_{i=0}^{N} \Delta T_i = \sum_{i=0}^{N} \frac{1}{v_i} \|\mathbf{x}_{i+1} - \mathbf{x}_i\|_2 \quad (6)$$

where v_i represents the wave velocity at position $\mathbf{x}_i = (x_i, z_i)$.

Using the Fermat's Principle of minimum time to characterize ray paths between two points, the following system of equations needs to be solved numerically (Červený, 2001):

$$\begin{cases} \dfrac{d\mathbf{x}}{ds} &= \dfrac{1}{|\mathbf{p}|}\mathbf{p}, \\ \dfrac{d\mathbf{p}}{ds} &= \vec{\nabla}\left(\dfrac{1}{v(\mathbf{x})}\right), \\ \dfrac{dT}{ds} &= \dfrac{1}{v(\mathbf{x})}. \end{cases} \quad (7)$$

where $\mathbf{p}(s)$ represents the slowness vector parameterized by the arc length s along the ray. Vector $\mathbf{p}$ is related to the velocity field v through the eikonal equation $|\mathbf{p}|^2 = 1/v^2(\mathbf{x})$. System (7) can be written in vector form as

$$\frac{d\mathbf{y}}{ds} = \mathbf{f}(s, \mathbf{y}), \quad (8)$$

where $\mathbf{y} = [\mathbf{x}, \mathbf{p}, T]$ and $\mathbf{f} = [\mathbf{p}/|\mathbf{p}|, -(1/v^2)\nabla v, 1/v]$. We discretize system (8) using the fourth-order Runge-Kutta method with step length Δs, *i.e.*, we consider $\mathbf{y}(n\Delta s) \approx \mathbf{y}_n$, where

$$\mathbf{y}_{n+1} = \mathbf{y}_n + \frac{1}{6}(\mathbf{k}_1 + 2\mathbf{k}_2 + 2\mathbf{k}_3 + \mathbf{k}_4), \quad (9)$$

$$\begin{cases} \mathbf{k}_1 = \Delta s \mathbf{f}(s_n, \mathbf{y}_n), \\ \mathbf{k}_2 = \Delta s \mathbf{f}(s_n + \frac{1}{2}\Delta s, \mathbf{y}_n + \frac{1}{2}\mathbf{k}_1), \\ \mathbf{k}_3 = \Delta s \mathbf{f}(s_n + \frac{1}{2}\Delta s, \mathbf{y}_n + \frac{1}{2}\mathbf{k}_2), \\ \mathbf{k}_4 = \Delta s \mathbf{f}(s_n + \Delta s, \mathbf{y}_n + \mathbf{k}_3). \end{cases}$$

Equation (9) is the basis for an algorithm that numerically calculates the trajectory of the seismic ray as well as the travel time of the seismic waves along these trajectories. The slowness vector is updated at each iteration of the Runge-Kutta method through the eikonal equation. For the initial condition, we assume the ray leaves a source point located at $\mathbf{x}_0$ with a prescribed take-off direction that defines the initial slowness $\mathbf{p}_0$, and set $T_0 = 0$.

In next section we will present tools that will allow us to estimate unknown parameters of the velocity field by parameterization of sigmoid functions by inverting the traveltimes.

Metropolis Hasting (MH) method

Let us introduce: a model vector $\mathbf{m}$ written as

$$\mathbf{m} = (m_1, m_2, \ldots, m_L)^T, \quad (10)$$

an observed data vector $\mathbf{d}_{obs}$, and the calculated vector data $\mathbf{d}_{calc}$ obtained directly from a synthetic model $\mathbf{m}$. To compute the misfit between the observed and the simulated data we use L_1-norm misfit given by

$$\phi(\mathbf{m}) = \|\mathbf{d}_{obs} - \mathbf{d}_{calc}(\mathbf{m})\|_1. \quad (11)$$

In our context, $\mathbf{m}$ represents the velocity field while

$$\begin{aligned} &\mathbf{d}_{obs} = (T_{obs}(\theta_1), T_{obs}(\theta_2), \ldots, T_{obs}(\theta_{NS}))^T, \\ &\mathbf{d}_{calc}(\mathbf{m}) = (T[\mathbf{m}](\theta_1), T[\mathbf{m}](\theta_2), \ldots, T[\mathbf{m}](\theta_{NS}))^T, \end{aligned} \quad (12)$$

where $T_{obs}(\theta_i)$ and $T[\mathbf{m}](\theta_i)$ are, respectively, the observed and the calculated traveltime for the ray with take-off angle θ_i, while N_r is the number of rays that reach the surface in both cases.

In order to compare the calculated data with the observed data we use the likelihood function

$$p(\mathbf{d}^{obs}|\mathbf{m}) = exp\left[-\frac{\phi^2(\mathbf{m})}{2N_s\sigma^2}\right]. \quad (13)$$

where N_s is the number of samples and σ is a standard deviation of the data error (Cho et al., 2017). The standard deviation σ is used as a fitting criterion for accepting or refusing in the MH method.

The MH also uses a proposal distribution $q(\mathbf{m},\mathbf{m}^*)$, which depends on the current state $\mathbf{m}$, to generate a new proposed sample $\mathbf{m}^*$ and a prior PDF uniformly distributed $p(\mathbf{m})$. Then, the values proposed are accept or rejected with probability

$$\nu(\mathbf{m},\mathbf{m}^*) = \min\left\{1, \frac{p(\mathbf{m}^*)p(\mathbf{d}^{obs}|\mathbf{m}^*)q(\mathbf{m},\mathbf{m}^*)}{p(\mathbf{m})p(\mathbf{d}^{obs}|\mathbf{m})q(\mathbf{m}^*,\mathbf{m})}\right\}. \quad (14)$$

If the proposal is not accepted, then the current value of $\mathbf{m}$ is retained: $\mathbf{m}^* = \mathbf{m}$. In our experiments we assume that the proposal distribution q is symmetric, $q(\mathbf{m},\mathbf{m}^*) = q(\mathbf{m}^*,\mathbf{m})$. In this case, the MH method reduces to a procedure called random walk.

In this inversion method, the random walk produces Markov chains after the first N iterations, which are discarded by a process called burn in period. Algorithm 1 provides a summary of this methodology.

Algorithm 1: MH algorithm for velocity field

Input: Build initial velocity field $\mathbf{m}^{(0)}$ by MC method
for $n \in \{1,\ldots,N_{mh}\}$ **do**
  $\xi^{(n-1)} \sim N(0,I)$;
  $\mathbf{m}^c \leftarrow \sqrt{1-\delta^2}\mathbf{m}^{(n-1)} + \delta\xi^{(n-1)}, \quad 0 < \delta \leq 1$;
  Acceptance Probability:

$$\nu(\mathbf{m}^c,\mathbf{m}^{n-1}) = \min\left\{1, \frac{p(\mathbf{m}^n)p(\mathbf{d}^{obs}|\mathbf{m}^n)}{p(\mathbf{m})p(\mathbf{d}^{obs}|\mathbf{m})}\right\};$$

  $u \sim U(0,1)$;
  if $u > \nu$ **then**
    Accept the velocity field: $\mathbf{m}^{(n)} \leftarrow \mathbf{m}^c$;
  else
    Reject the velocity field: $\mathbf{m}^{(n)} \leftarrow \mathbf{m}^{(n-1)}$;
  end
end

Results and discussion

In the following experiments, the dimensions of the domain are fixed in $L_x = 9.4$ km and $L_z = 3.0$ km for all examples. In this case the rays depart from $\mathbf{x_0} = [\mathbf{x_0}, \mathbf{z_0}]$ with take-off angle θ with respect to the z-axis, *i.e.,* $\mathbf{p_0} = [\sin(\theta), \cos(\theta)]/\mathbf{v_0}$. In the experiments we considered 1000 samples in the MH method after a burn in period of 100 samples, totaling 1100 realizations in the inverse process.

Horizontally layered model (M_1)

Let us choose as target model an elementary one-dimensional model of three horizontal layers of thickness $L = 0.75$ km and velocities $v_1 = 2.0$ km/s, $v_2 = 2.5$ km/s, and $v_3 = 3.0$ km/s with a single surface source at the origin (Oliveira et al., 2020). The velocity below the third layer is $v_4 = 4.0$ km/s. The target model and reference ray paths are displayed Fig. 2.

This model allows travel times to be calculated analytically. For the purpose of comparison with the numerical solution, the arrival reflection locations $x^{(i)}$ and traveltimes $T^{(i)}$ ($i = 1,2,3$) for an arbitrary take-off angle θ are defined by

$$x^{(i)} = 2L\sum_{k=1}^{i}\tan\theta_k, \quad T^{(i)} = 2L\sum_{k=1}^{i}\frac{\sec\theta_k}{v_k}, \quad (15)$$

where $\theta_1 = \theta$ and $\theta_i = \sin^{-1}((v_i/v_{i-1})\sin\theta_{i-1})$ for $i = 2,3$.

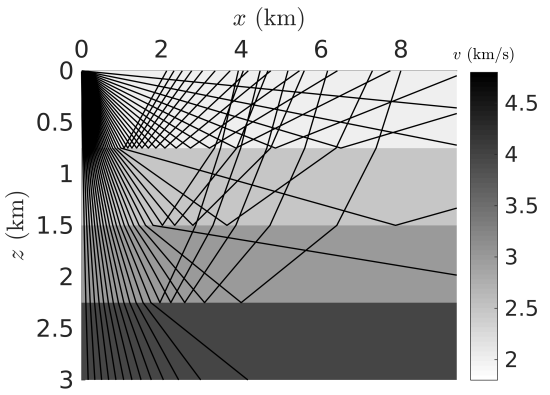

Figure 2: Reference solutions for the horizontally layered model (M_1): paths of 40 rays with take-off angles uniformly distributed in $[0°, 90°[$.

In this example the forward responses obtained by the MH method were compared with the Very Fast Simulated Annealing (VFSA) which is also a global optimization method used for finding the global minimum of a function (see, e.g., Oliveira et al., 2018). In this case, the initial and final temperatures are $T_0 = 1$ and $T_f = 0.01$, whereas the parameter c is defined by average rate of change of temperature in log scale given by $\Delta t = 0.01$. Here, the number of models tested by temperature is 100.

In the following, we compare ray paths obtained with MH and VFSA (Fig. 3) with the target solution given by Fig. 2. The MH inversion with slope parameter a = 10 yields smoothed velocity fields and ray paths (Fig. 3a). A similar result was obtained by the VFSA method and therefore it was omitted here. However there is a good fit with the observed data for both methods when parameter a = 100 (see Figs. 3b-3c). In addition, Table 1 shows the superiority of MH over VFSA. In both parameters, the results presented by misfit and CPU time had lower values in MH method.

The travel times of the sigmoidal representation selected in Fig. 3 are shown in Fig. 4. The straight lines are the travel times obtained by the equation (15). We can infer that the results from MH method have acceptable fitness

a	Method	Misfit	CPU
10	MH	209.0455	1619.61
	VFSA	233.5181	164331
100	MH	53.6060	1133.93
	VFSA	103.2884	158661

Table 1: Misfit and CPU time for model M_1 considering MH and VFSA methods.

due to its low relative error. It is also important to note that in a = 100, the VFSA method obtained better results than the MH in relation to travel times, however, the MH is able effectively generate a velocity field profile where the rays were reflected in the third layer.

High-Velocity Intrusion Model (M_2)

In the next synthetic test, we consider a representation of velocity field with intrusion of high velocity at the center of the domain. Let us consider a domain with having 3 rows and 4 columns totaling 12 coefficients to determine. The velocities vary from 1.5 km/s to 5.5 km/s (see Fig. 5), establishing the target model. Similar study involving interpolation Haar functions and the Metropolis algorithm was carried out in Cerqueira et al. (2016). The arrangement consists of one source located at $(4.65, 0)$ km with take-off angle θ uniformly distributed in $[-45°, 45°]$.

Figure 6 shows the ray paths from sigmoidal representations with inverted model assuming parameters a = 10 and a = 100. As in Fig. 4, we employ 40 rays to illustrate the ray trajectories through the model. It should be noted that the solution by MH method manged to highlight the intrusion zone. Note at a = 100 we got better results in the velocity field. However, in both slopes parameters, the velocity field has been able to register reflections only near the source and consequently travel times have been discarded along the edges of the domain (Fig. 7).

Conclusions

Usually seismic models are described by two parameters of diferent nature: wave velocities on rocks and interfaces between layers. Such situation is a source of ambiguity in travel time seismic inversion procedures. A strategy to mitigate such problem is to consider such model as an unique object: a velocity field parameterized by a sigmoidal series that is able to simulate geometrical discontinuities at interfaces by a continuous and fast variation. Sigmoidal function representation make stronger the coupling or relationship between lenghts and velocities, reducing, then, model parameters indeterminancy. Such advantages are explored and illustrated in this proposed work in order to improve results as shown in the numerical inversion performed experiments.

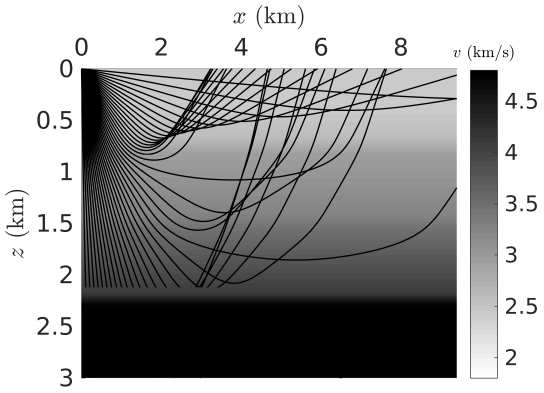

(a) MH, a = 10

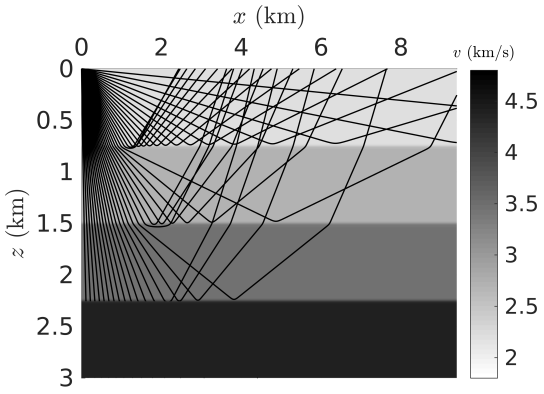

(b) MH, a = 100

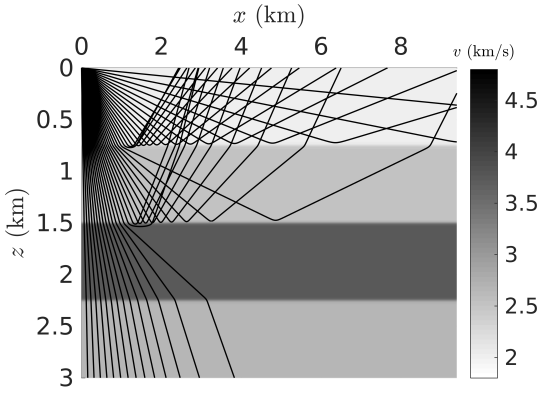

(c) $VFSA$, a = 100

Figure 3: Velocity fields and ray paths obtained by inverting the travel times of the rays shown in Fig. 4: (a) MH with a = 10; (b) MH with a = 100; (c) VFSA with a = 100.

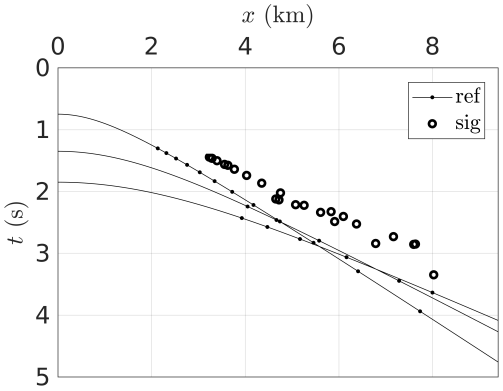

(a) MH, a = 10

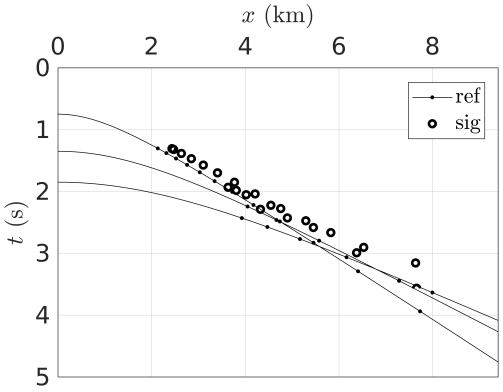

(b) MH, a = 100

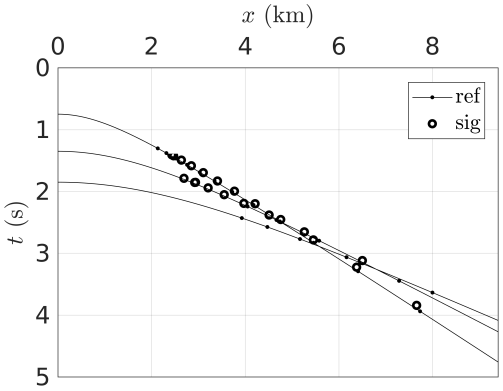

(c) $VFSA$, a = 100

Figure 4: Comparison between observed (ref) and calculated (sig) traveltimes in the horizontally layered model (M_1) considering slope parameters a = 10 and a = 100: global methods MH (a)-(b) and VFSA (c). The sigmoidal parameterization with a = 100 had a good approximation with the MH while the VFSA performed better, however with a very high CPU time.

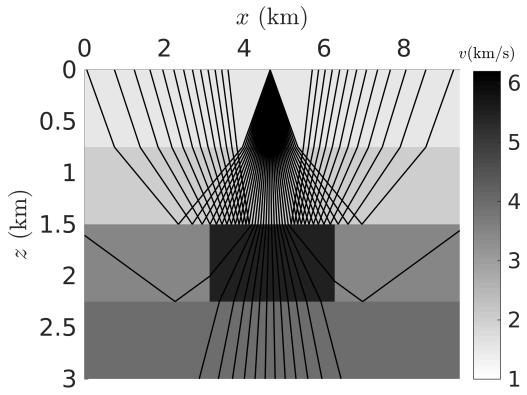

Figure 5: Reference solutions for the high-velocity intrusive model (M_2): paths of 40 rays with take-off angles uniformly distributed in $[-45°, 45°]$.

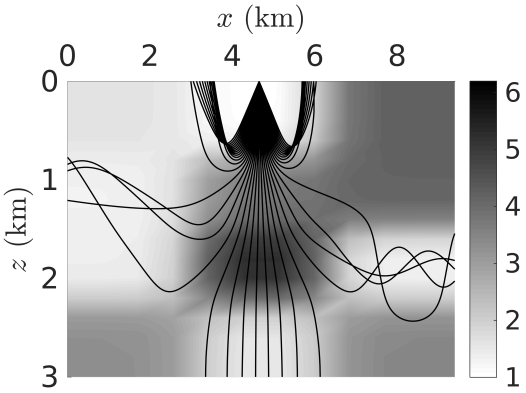

(a) a = 10

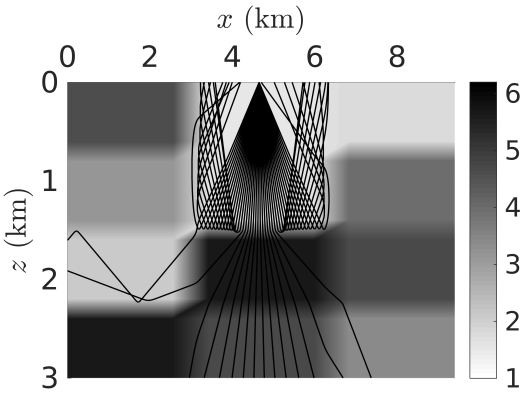

(b) a = 100

Figure 6: Ray paths from sigmoidal representations of the inverted intrusive model (M_2) with $a = 10$ (a) and $a = 100$ (b).

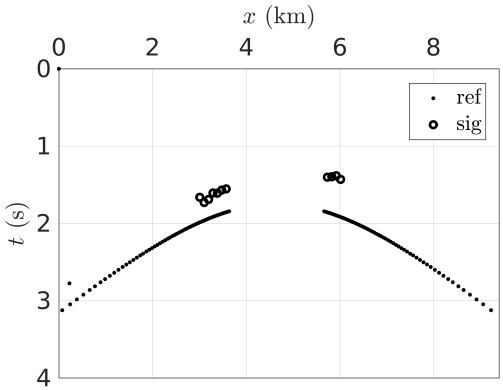

(a) a = 10

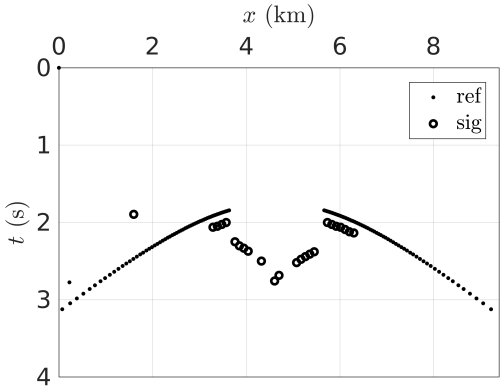

(b) a = 100

Figure 7: Comparison between observed (ref) and calculated (sig) traveltimes of 200 rays in the high-velocity intrusive model (M_2) considering slope parameters a = 10 (a) and a = 100 (b). The calculated traveltimes have been found by the MH method.

References

Azevedo, J. S., G. S. Cardoso, and L. Schnitman, 2014, An adaptive Monte Carlo Markov Chain method applied to the flow involving self-similar processes in porous media: Journal of Porous Media, **17**.

Belhadj, J., T. Romary, A. Gesret, M. Noble, and B. Figliuzzi, 2018, New parameterizations for bayesian seismic tomography: Inverse Problems, **34**, 065007.

Cerqueira, A. G., W. M. Figueiró, and P. E. M. Cunha, 2016, Seismic tomography using metropolis method of velocity fields parameterized by haar wavelet series: Brazilian Journal of Geophysics, **34**, 251–260.

Červený, V., 2001, Seismic Ray Theory: Cambridge University Press.

Cho, Y., D. Zhu, and R. Gibson, 2017, 3D transdimensional Markov-chain Monte Carlo seismic inversion with uncertainty analysis, *in* SEG Technical Program Expanded Abstracts 2017: Society of Exploration Geophysicists, 607–611.

Costarelli, D., and R. Spigler, 2013, Constructive approximation by superposition of sigmoidal functions: Analysis in Theory and Applications, **29**, 169–196.

Evensen, A. K., and M. Landrø, 2010, Time-lapse tomographic inversion using a Gaussian parameterization of the velocity changes: Geophysics, **75**, U29–U38.

Kissling, E., S. Husen, and F. Haslinger, 2001, Model parametrization in seismic tomography: a choice of consequence for the solution quality: Physics of the Earth and Planetary Interiors, **123**, 89–101.

Michelini, A., and T. V. McEvilly, 1991, Seismological studies at Parkfield. I. Simultaneous inversion for velocity structure and hypocenters using cubic B-splines parameterization: Bulletin of the Seismological Society of America, **81**, 524–552.

Oliveira, S., J. Azevedo, and M. Porsani, 2018, A numerical viscoelastic model of ground response assimilating pore-water pressure measurements.: Bollettino di Geofisica Teorica ed Applicata, **59**.

Oliveira, S. P., J. S. Azevedo, W. M. Figueiró, R. A. Guimarães, W. J. Silva, and A. de Oliveira, 2020, Representation of discontinuous seismic velocity fields by sigmoidal functions for ray tracing and traveltime modelling: Geophysical Journal International, **224**, 435–448.

Tikhotskii, S., I. Fokin, and D. Y. Schur, 2011, Traveltime seismic tomography with adaptive wavelet parameterization: Physics of the Solid Earth, **47**, 326–344.

Tong, P., D. Yang, and X. Huang, 2019, Multiple-grid model parametrization for seismic tomography with application to the San Jacinto fault zone: Geophysical Journal International, **218**, 200–223.